

Exceptional point and hysteresis in perturbations of Kerr black holes

João Paulo Cavalcante,^{1,*} Maurício Richartz,^{2,†} and Bruno Carneiro da Cunha^{1,‡}

¹*Departamento de Física, Universidade Federal de Pernambuco, 50670-901, Recife, Brazil*

²*Centro de Matemática, Computação e Cognição,*

Universidade Federal do ABC (UFABC), 09210-580, Santo André, São Paulo, Brazil

We employ the isomonodromic method to study linear scalar massive perturbations of Kerr black holes for generic scalar masses $M\mu$ and generic black hole spins a/M . We find that the longest-living quasinormal mode and the first overtone coincide for $(M\mu)_c \simeq 0.3704981$ and $(a/M)_c \simeq 0.9994660$. We also show that the longest-living mode and the first overtone change continuously into each other as we vary the parameters around the point of degeneracy, providing evidence for the existence of a geometric phase around an exceptional point. We interpret our findings through a thermodynamic analogy.

Introduction – Black holes, according to the uniqueness theorems of General Relativity [1, 2], are remarkably simple objects. In vacuum, the most general black hole is described by the Kerr spacetime and depends only on two parameters: its mass M and its specific angular momentum a [3, 4]. Black holes are also regarded as thermodynamic systems, with a temperature proportional to their surface gravity and an entropy proportional to their surface area [5, 6].

When a black hole is disturbed, it rings down through quasinormal modes (QNMs) [7–10], characterized by complex frequencies. The real part of ω relates to the wavelength of the oscillation, while the inverse of the imaginary part of ω corresponds to the characteristic decay time of the QNM. In the linear regime, each frequency ω depends not only on the black hole itself but also on defining parameters of the perturbation, such as the azimuthal number m , the orbital number ℓ , and the overtone number n . Black hole spectroscopy uses the QNM spectrum to infer the parameters that specify the black hole [11–15]. This method of describing the ringdown phase of black hole merger events detected by gravitational wave observatories has become particularly important in the last decade [16–19].

The near extremal regime $a/M \rightarrow 1$ of a Kerr black hole provides critical insights into the nature of classical [20–38] and quantum gravity [39–48]. In particular, scalar QNMs can be classified into *damped modes* (DM), for which $\text{Im}(\omega)$ approaches a nonzero finite value in the extremal limit and *undamped modes*, known as *zero-damping modes* (ZDM), which are characterized by $\text{Re}(\omega) \rightarrow m/(2M)$ and $\text{Im}(\omega) \rightarrow 0$ as extremality is approached [49–57]. In fact, as the spin of a black hole approaches the extremal limit, the imaginary part of different overtones may cross each other [53, 54]. Furthermore, the accumulation of an infinite number of ZDMs at the real axis has been associated with the horizon instability of extremal black holes [58–60].

Massive scalar fields around rotating black holes have been investigated not only as theoretical laboratories and testbeds for their electromagnetic and gravitational counterparts, but also in astrophysical scenarios. They are

potentially relevant to the formation of scalar clouds, driven by superradiant instabilities [61–64], around rotating black holes [65, 66], as well as to the prospect of their use as particle detectors [67–69].

In this letter we systematically explore the parameter space of massive scalar perturbations in Kerr black holes and identify a point of degeneracy where the fundamental QNM and its first overtone coincide. We further identify a curve in the parameter space, emanating from the degeneracy point, where the decay times of these QNMs are the same. We also demonstrate that the QNMs transform into each other when this curve is crossed in the parameter space. This unveils the existence of hysteresis in Kerr black holes: the result of following adiabatically a QNM in parameter space will depend on the path taken.

We interpret our findings in terms of exceptional points of non-hermitian systems [70], whose far-reaching implications have been investigated in different dissipative systems, specially in optics and photonics [71–74]. Finally, we draw an analogy of our results with the phase space of thermodynamic systems that undergo phase transitions, where phenomena such as critical points and level-crossing are well established.

Throughout this work we use natural units $G = c = \hbar = 1$.

Linear perturbations – Linear perturbations of a scalar field of mass μ around a Kerr black hole are described by the Klein-Gordon equation. In Boyer-Lindquist coordinates, the equation is separated into radial and angular equations [75]. The radial part is

$$\partial_r(\Delta \partial_r R) + \left[\frac{[\omega(r^2 + a^2) - am]^2}{\Delta} - \lambda - \mu^2 r^2 \right] R = 0, \quad (1)$$

where $\Delta = r^2 - 2Mr + a^2 = (r - r_+)(r - r_-)$. The roots r_+ and r_- correspond, respectively, to the event horizon and to the Cauchy horizon of the black hole. The angular velocities Ω_{\pm} and the temperatures T_{\pm} associated with the horizons r_{\pm} are given by

$$\Omega_{\pm} = \frac{a}{2Mr_{\pm}}, \quad 2\pi T_{\pm} = \frac{r_{\pm} - r_{\mp}}{4Mr_{\pm}}. \quad (2)$$

The separation constant $\lambda \equiv \lambda_{\ell, m}$ depends on the angular quantum numbers ℓ and m and its computation stems from a Sturm-Liouville (eigenvalue) problem of the angular equation.

In terms of $u = \cos \theta$, the angular equation is

$$\partial_u [(1 - u^2)\partial_u S] + \left(\frac{m^2}{1 - u^2} - c^2 u^2 - \Lambda \right) S = 0, \quad (3)$$

where $c = a\sqrt{\omega^2 - \mu^2}$ and $\Lambda = \lambda + 2am\omega - a^2\omega^2$. Regularity at the poles (corresponding to $u = \pm 1$) implies that the angular solutions are spheroidal harmonics $S(\theta) = S_{\ell m}(\theta; c)$, with parameters ℓ and m satisfying the constraints $\ell \in \mathbb{N}$, $m \in \mathbb{Z}$ and $-\ell \leq m \leq \ell$ [76, 77].

The angular and radial equations can be cast as the *confluent Heun equation* (CHE) [78, 79],

$$\frac{d^2 y}{dz^2} + \left[\frac{1 - \theta_0}{z} + \frac{1 - \theta_t}{z - t} \right] \frac{dy}{dz} - \left[\frac{1}{4} + \frac{\theta_\star}{2z} + \frac{tc_t}{z(z - t)} \right] y = 0, \quad (4)$$

which is defined for generic complex parameters $t, c_t, \{\theta_k\} = \{\theta_0, \theta_t, \theta_\star\}$, and a complex independent variable z . For convenience, we also define $\{\theta_k\}_- = \{\theta_0, \theta_t - 1, \theta_\star + 1\}$. In the theory of ordinary differential equations on the complex plane, the CHE is characterized by regular singular points at $z = 0$ and $z = t$, where the asymptotic behavior of the solution is polynomial, and an irregular singular point at $z = \infty$, where the asymptotic solutions are exponentials [80, 81].

In particular, the CHE parameters for the angular equation (3) are

$$\begin{aligned} \theta_0 &= -m, & \theta_t &= m, & \theta_\star &= 0, & \alpha &= \sqrt{\omega^2 - \mu^2}, \\ t &= -4a\alpha, & tc_t &= \lambda + 2(1 - m)a\alpha + a^2\alpha^2, \end{aligned} \quad (5)$$

while the CHE parameters for the radial equation (1) are

$$\begin{aligned} \theta_0 &= \frac{-i}{2\pi T_-} (\omega - m\Omega_-), & \theta_t &= \frac{i}{2\pi T_+} (\omega - m\Omega_+), \\ \theta_\star &= \frac{2iM(2\omega^2 - \mu^2)}{\alpha}, & t &= 2i\alpha(r_+ - r_-), \\ tc_t &= \lambda + r_+^2\mu^2 - (3a^2 + r_-^2 + 3r_+^2)\omega^2 \\ &\quad + i(r_- - r_+ - 2iam + 2i(a^2 + r_+^2)\omega)\alpha \\ &\quad + i\frac{M(2\omega^2 - \mu^2)}{\alpha} + \frac{M^2(2\omega^2 - \mu^2)^2}{\alpha^2}. \end{aligned} \quad (6)$$

QNMs and the isomonodromic method – QNMs correspond to solutions of the radial equation (1) that are purely ingoing at the event horizon and purely outgoing far away from the black hole. The calculation of QNM frequencies is typically performed by substituting appropriate Frobenius series expansions into the angular and radial equations and solving the resulting recurrence relations using continued fractions. Although this technique, known as *Leaver's method* [82, 83], enjoys fast convergence in general, it breaks down in the extremal case

$a = M$ due to the fact that the event horizon becomes an irregular singular point of the differential equation. There are extensions proposed to deal with this issue, with varying degrees of success [28, 35, 56, 57].

One of the alternatives, known as the *isomonodromic method* [35, 57], relies on the fact that the boundary-value problems associated with the angular and radial equations can be cast in terms of the *composite monodromy parameters*, which in turn dictate the analytic continuation of the solutions of the CHE as one considers paths on the complex plane encompassing the singular points of the equation. The main advantage of the method is the analytic control it provides over the dependence of the composite monodromy parameters on the parameters of the equation. This control ensures a smooth limit when determining QNM frequencies in the extremal case.

The map between the composite monodromy parameters, which we denote by σ and η , and the parameters of the CHE is known in mathematics literature as the *Riemann-Hilbert map* (RH map). In the isomonodromy method this map is solved using the *Painlevé V transcendent* [84]. Schematically, the RH map translates into the following pair of equations

$$\tau_V(\{\theta_k\}; \sigma, \eta; t) = 0, \quad (7a)$$

$$t \frac{\partial}{\partial t} \log \tau_V(\{\theta_k\}_-; \sigma - 1, \eta; t) - \frac{\theta_0(\theta_t - 1)}{2} = tc_t, \quad (7b)$$

where τ_V is the *tau-function* of Painlevé V, a type of special function required to solve the class of boundary-value problems associated with black hole QNMs.

Given a choice of physical parameters ($a/M, M\mu, \ell, m$), the monodromy parameter σ can be determined through a Floquet-type solution of (4),

$$y(z) = e^{-\frac{1}{2}z} z^{\frac{1}{2}(\sigma + \theta_0 + \theta_t) - 1} \sum_{n=-\infty}^{\infty} C_n z^n. \quad (8)$$

Substituting the series above into (4) produces a 3-term recursion relation for C_n , which can be solved as in Leaver's method, yielding

$$\sigma = \sigma(\{\theta_k\}, c_t, t). \quad (9)$$

The parameter σ determined this way solves (7b). In fact, σ parametrizes the complex phase of (8) as one continues it analytically over a path encompassing the singular points $z = 0$ and $z = t$. In contrast, the interpretation of the monodromy parameter η is quite involved [85]. For our purposes, we can just define the parameter by formally inverting the zero condition for τ_V (7a):

$$\eta = \eta(\{\theta_k\}, \sigma, t), \quad (10)$$

where σ can be computed in terms of the CHE parameters by (9). For a detailed discussion, we refer to [86].

The usefulness of the RH map stems from the fact that boundary value problems involving the CHE can be solved by placing suitable constraints on σ and η . In particular, the boundary value problem of the angular equation (3), *i.e.* regularity at the poles, is solved by the requirement that the parameter σ , as given in (9), satisfies

$$\sigma = \theta_0 + \theta_t + 2(\ell + 1) = 2(\ell + 1), \quad \ell = 0, 1, 2, \dots, \quad (11)$$

where we have used θ_0 and θ_t as defined in (5), and related the parameter σ to the angular quantum number ℓ . This equation relates the eigenvalues λ and ω associated with the QNM problem. For $a\alpha \ll 1$, the expansion of $\lambda = \lambda(\omega)$ coincides with the usual expansion for the eigenvalue of the spheroidal harmonics [77]. Similarly, the asymptotic behavior for large $a\alpha$ can also be determined using monodromy techniques [85, 87].

Concerning the radial equation, QNMs are associated with boundary conditions which are purely ingoing at $r = r_+$ and purely outgoing at $r = \infty$. As discussed in more detail in [86], the mapping from r in (1) to z in (4) depends on α , and for $\text{Re } \alpha > 0$ the QNM boundary condition translates to

$$e^{\pi i \eta} = e^{-\pi i \sigma} \frac{\sin \frac{\pi}{2}(\theta_* + \sigma)}{\sin \frac{\pi}{2}(\theta_* - \sigma)} \times \frac{\sin \frac{\pi}{2}(\theta_t + \theta_0 + \sigma) \sin \frac{\pi}{2}(\theta_t - \theta_0 + \sigma)}{\sin \frac{\pi}{2}(\theta_t + \theta_0 - \sigma) \sin \frac{\pi}{2}(\theta_t - \theta_0 - \sigma)}, \quad (12)$$

with $\{\theta_k\}$ defined in (6). After using (9) and (10), the equation above yields another constraint between the separation constant λ and the QNM frequency ω .

Numerical Implementation – QNMs are characterized by the integers ℓ and m and depend on two dimensionless parameters, the normalized mass of the field $M\mu$ and the normalized angular momentum of the black hole a/M . We solve the coupled equations (11) and (12) numerically to determine the angular eigenvalue λ and the radial eigenvalue (*i.e.* the QNM frequency) ω . For a given set of parameters, there is a countably infinite number of frequencies ω , indexed by the non-negative integer n , that solve the equations. When $M\mu = a/M = 0$, we classify these infinitely many QNMs according to the magnitude of the imaginary part of their frequency. In other words, $n = 0$ refers to the longest living mode and $n = 1$ to the first overtone when the field is massless and the black hole is nonrotating.

In this letter, we investigate the $\ell = m = 1$ QNMs across the two-dimensional parameter space $(a/M, M\mu)$, focusing on the question of what is the longest-living mode as the mass of the scalar field and the spin of the black hole vary. At generic points, we follow adiabatically the roots of the RH map with increments in $M\mu$ of order 10^{-3} and increments in a/M of order 10^{-5} . Near the exceptional point (see below) and near the extremal limit, we reduce the increments by 2 or 3 orders of magnitude.

We carry out the isomonodromic method using a **Julia** implementation of the Fredholm determinant formulation of τ_V , truncated at $N_f = 64$ levels. The determination of the parameter σ employs a continued fraction approximant at $N_c = 128$ levels. We use the **ArbNumerics** implementation for arbitrary precision arithmetic and dense matrix determinant calculations, working at 384 digits. When possible, we used both small and large t expansions to ensure numerical stability of at least 12 digits. Numerical codes and datasets are publicly available [88].

Exceptional point and “level crossing” – We reveal the existence of an exceptional point in the parameter space where the fundamental QNM and its first overtone degenerate. In perturbation theory, exceptional points arise due to non-hermiticity of linear operators and, hence, are also known as non-hermitian degeneracies [70]. Even though the effective potentials describing perturbations of Kerr black holes, such as the one associated with the radial equation (1), have been recognized as non-hermitian for a long time, to the best of our knowledge exceptional points had not yet been identified in black hole physics.

By exploring the frequencies of the fundamental QNM and its first overtone as extremality is approached at different values of the scalar field mass, we have identified a transition from ZDMs to DMs. Within numerical accuracy, we have found that, for $(M\mu)_c \simeq 0.3704981$, the $n = 0$ mode changes its behavior as we increase a/M . For $M\mu < (M\mu)_c$, the $n = 0$ mode is a ZDM, and its frequency approaches $m/2M$ in the extremal limit. Conversely, for $M\mu > (M\mu)_c$, the mode is a DM, meaning that the imaginary part of its frequency does not approach zero as $a/M \rightarrow 1$. The sudden change of behavior is shown in Fig. 1 as a/M varies towards extremality. The same transition is observed in Fig. 2, where we vary the mass of the scalar field for a selection of black hole spins around the critical value $(a/M)_c$. As both figures unveil, at the critical point defined by $M\mu = (M\mu)_c$ and $a/M = (a/M)_c \simeq 0.9994660$, the fundamental QNM develops a cusp. We remark that a similar behavior was observed for charged massless perturbations of Reissner-Nordström black holes [89].

The fact that the $n = 0$ modes become DMs for $M\mu > (M\mu)_c$ when the black hole is spinning sufficiently fast implies that they may not be the longest-living modes at every point of the parameter space. In fact, by following the $n = 0$ and the $n = 1$ QNMs throughout the parameter space, we have observed that their frequencies coincide at the critical point, which is thus understood as an exceptional point of a non-hermitian system. One of the exotic features of the exceptional point is shown in Fig. 3, where we plot both QNMs as a function of $M\mu$ for $a/M \lesssim (a/M)_c$ and $a/M \gtrsim (a/M)_c$. As the spin increases through the critical value, we observe that the QNMs degenerate and transform into each other. The parameter space $(a/M, M\mu)$ is shown in Fig. 4, where

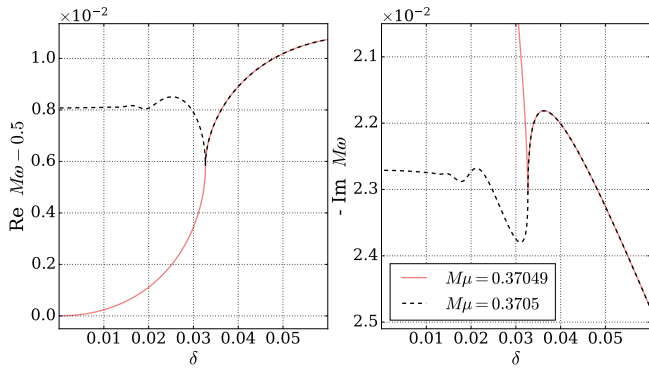


FIG. 1. The $n = 0$ QNM frequency as a function of $\delta = \cos^{-1}(a/M)$. The solid line shows the behavior for $M\mu \lesssim (M\mu)_c$, whereas the dashed line corresponds to $M\mu \gtrsim (M\mu)_c$. We observe the exceptional point at $\delta = \delta_c \simeq 0.0326823$.

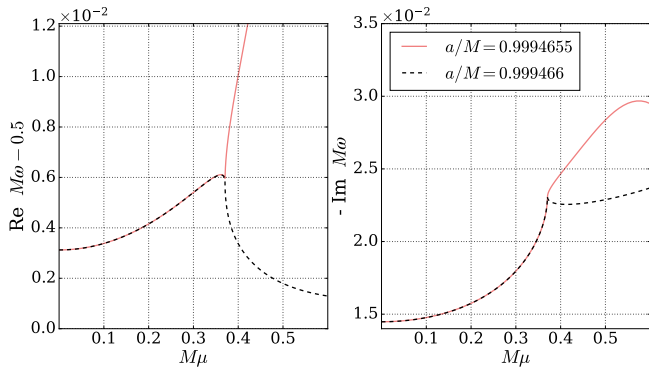


FIG. 2. The $n = 0$ QNM as a function of $M\mu$. The solid line corresponds to $a/M < (a/M)_c$, while the dashed curve corresponds to $a/M > (a/M)_c$. We observe the exceptional point at $M\mu = (M\mu)_c \simeq 0.3704981$.

the exceptional point is represented as a star. We have also identified a “curve of coexistence” emerging from the critical point, represented as a dashed curve, where the imaginary parts of the frequencies for the $n = 0$ and the $n = 1$ modes coincide. In the accompanying paper [86] we characterize the coexistence curve with greater detail.

Note the curve separating the shaded (green) and white regions, defined by $\text{Re } \alpha = 0$ for the $n = 0$ modes, above which the QNM boundary condition no longer follows Eq. (12). Extending the QNM analysis into the white region is beyond the scope of this letter, but some insights are discussed in [86]. When the QNMs are adiabatically deformed along a path that intersects the coexistence curve, such as the path AD in Fig. 4, the longest-living mode switches to the second longest-living mode, and vice-versa.

Geometric phase and hysteresis – So far we used $n = 0$ and $n = 1$ to refer to the spectrum of QNMs as ordered by their imaginary parts in the massless

Schwarzschild configuration. The presence of an exceptional point means that following adiabatically either mode may yield different results depending on the path taken in parameter space. The path dependence establishes the existence of non-contractible curves in parameter space and ensures the existence of the exceptional point, whose numerical evidence we discussed above.

To illustrate this, we have adiabatically followed some of the modes around a closed path in parameter space containing the exceptional point. We have found that, even if the starting and ending points of the parameter space trajectory coincide, the final QNM frequency differs from the corresponding initial value, signalling the existence of a non-trivial geometric phase. Explicitly, consider the rectangle $ABCD$ shown in Fig. 4, whose vertices $(a/M, M\mu)$ are $A = (0.999, 0.45)$, $B = (0.999, 0.3)$, $C = (0.9999, 0.3)$ and $D = (0.9999, 0.45)$. We start with the longest-living mode at A , whose frequency is $\omega_\alpha(A) = 0.514974 - 0.026418i$. Changing the parameters continuously along the path $ABCD$, and thus avoiding the coexistence curve, yields the longest-living mode at D , with frequency $\omega_\alpha(D) = 0.500386 - 0.009456i$. On the other hand, deforming the QNM through the straight line AD , and thus crossing the coexistence curve, results in the second longest-living mode at D , with frequency $\omega_\beta(D) = 0.514827 - 0.026255i$. If we repeat the procedure starting with the second longest-living mode at A , whose frequency is $\omega_\beta(A) = 0.503306 - 0.032998i$, the results are reversed: the straight line leads to the longest-living mode at D , with frequency $\omega_\alpha(D)$, whereas the path that avoids the coexistence curve leads to the second longest-living mode at D , with frequency $\omega_\beta(D)$. To corroborate our findings, we also implemented Leaver’s method [88], as outlined in [63, 90–93], and obtained the same numerical results.

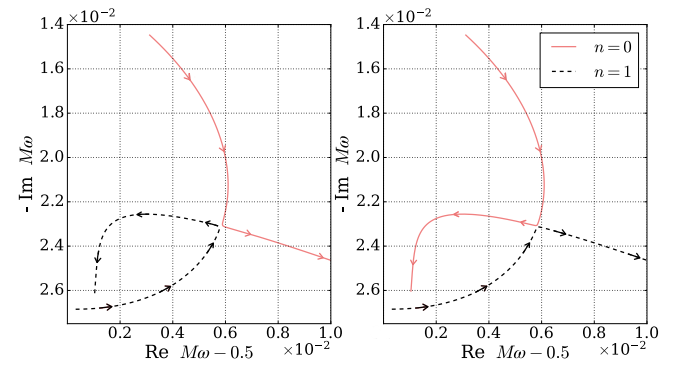


FIG. 3. The $n = 0$ and $n = 1$ QNMs as a function of $M\mu$ for $a/M \lesssim (a/M)_c$ (left) and $a/M \gtrsim (a/M)_c$ (right). The arrows denote the direction of increasing $M\mu \in [0.0, 0.8]$. At $\{a/M, M\mu\} = \{(a/M)_c, (M\mu)_c\}$, the QNMs become degenerate and transform into each other, resembling the level crossing behavior of thermodynamical systems.

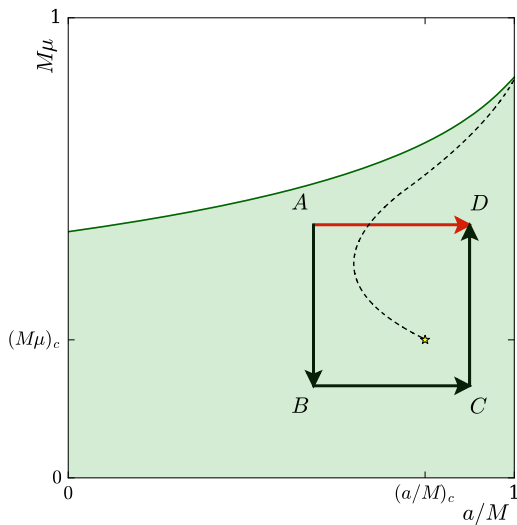


FIG. 4. Schematic representation of the parameter space associated with $\ell = m = 1$ massive scalar perturbations in Kerr black holes. The star corresponds to the exceptional point where the $n = 0$ and the $n = 1$ QNMs are degenerate. The dashed line corresponds to the coexistence curve where the decay rates of these QNMs are equal. Deformations of a QNM along the paths AD and $ABCD$ yield different results, characterizing the occurrence of hysteresis. The curve separating the shaded (green) and white regions is characterized by $\text{Re } \alpha = 0$ for the $n = 0$ modes.

Discussion – We have gathered strong evidence for the existence of exceptional points and geometric phases associated with linear massive scalar perturbations of near extremal Kerr black holes. To support these conclusions, we have examined the dependence of the QNM frequency on the spin of the black hole and on the mass of the scalar field, in a way that mimics thermodynamic systems. We have presented a short discussion of the isomonodromic method, focusing on the existence of a degeneracy and the possibility of hysteresis for the $\ell = m = 1$ modes. The complete technical details and results for general quantum numbers are provided in the companion paper [86], where we discuss QNM frequencies beyond their behaviour around the exceptional point.

We conclude this letter by interpreting our results through the lens of statistical mechanics. The Fredholm determinant formulation of the Painlevé V tau-function [94] expresses τ_V as

$$\tau_V = \Upsilon \det(\mathbb{1} - K(\omega)), \quad (13)$$

where K is an integral operator and Υ is a function of t that vanishes only at the critical points $t = 0$ and $t = \infty$ (corresponding to $\omega = 0$ and $\omega = \infty$, respectively). The specific forms of Υ and K are not essential for this discussion and can be found in [57]. The key aspect is that identifying non-trivial zeros of τ_V , which are associated with the calculation of the QNM frequencies through (9)-

(12), reduces to computing zeros of the determinant in (13).

At this point, there is a clear analogy between solving for the zeros of the determinant in (13) and solving the secular equation to find the eigenvalues of the transfer matrix in a statistical mechanical system. Furthermore, describing the ringdown of the black hole through the longest-living frequency of $K(\omega)$ can be understood as an analogous procedure to keeping the largest eigenvalue of the transfer matrix. In statistical mechanics, the latter procedure amounts to computing the free energy of the system in the thermodynamical limit.

We posit that the existence of the exceptional point and hysteresis phenomena we reported for Kerr black holes is analogous to the behavior of a thermodynamical system near a critical point. The critical point is the end of a curve of coexistence between phases, where there is a discontinuity of the free energy of the system. Likewise, in our coexistence curve the imaginary parts of the frequency match but the real part does not. In the thermodynamical system, continuing the curve beyond the critical point reveals a cross-over where the phases transmute smoothly into one another, without any apparent discontinuity. We observe the same behavior by taking the $ABCD$ path in Fig. 4, as if $K(\omega)$ were a non-linear version of the transfer matrix of a statistical mechanical system.

Level-crossing and cross-overs are generic features of phase transitions in thermodynamics, as demonstrated in standard textbook treatments of the van der Waals fluid [95]. We have presented compelling evidence, through the specific example of massive scalar fields in Kerr black holes, that gravitational systems can display the same behavior. Although localized in physical configuration space, these phenomena undoubtedly impact the ringdown phase and the overall behavior of massive fields when the relevant conditions are met. These topics present exciting opportunities for future research.

It is remarkable that the critical mass aligns with the regime where superradiant instabilities are most efficient, *i.e.* $(M\mu)_c \sim \mathcal{O}(1)$ [69]. In particular, putative bosonic condensates growing from these instabilities can emit gravitational waves through several channels (*e.g.* continuous emission arising from annihilation of the boson field or level transitions between states with different overtone numbers). Such processes (superradiant instabilities and gravitational wave emission) change the mass and the spin of the black hole, drawing paths in the parameter space (as in Fig. 4) that may cross a coexistence curve and encompass an exceptional point.

Note added. After completing this work, we learned of a recent preprint by Motohashi [96], which interprets an avoided crossing [97–99] near a degeneracy point as the mechanism underlying resonances between gravitational QNMs.

Acknowledgements – The authors thank André Lima

for comments and suggestions on the manuscript. M. R. acknowledges partial support from the Conselho Nacional de Desenvolvimento Científico e Tecnológico (CNPq, Brazil), Grant 315991/2023-2, and from the São Paulo Research Foundation (FAPESP, Brazil), Grant 2022/08335-0.

* joao.paulocavalcante@ufpe.br

† mauricio.richartz@ufabc.edu.br

‡ bruno.ccunha@ufpe.br

- [1] M. Heusler, *Black Hole Uniqueness Theorems*, Cambridge Lecture Notes in Physics (Cambridge University Press, 1996).
- [2] P. T. Chrusciel, J. Lopes Costa, and M. Heusler, Stationary Black Holes: Uniqueness and Beyond, *Living Rev. Rel.* **15**, 7 (2012), arXiv:1205.6112 [gr-qc].
- [3] R. P. Kerr, Gravitational field of a spinning mass as an example of algebraically special metrics, *Phys. Rev. Lett.* **11**, 237 (1963).
- [4] D. L. Wiltshire, M. Visser, and S. M. Scott, *The Kerr spacetime: Rotating black holes in general relativity* (Cambridge University Press, 2009).
- [5] J. M. Bardeen, B. Carter, and S. W. Hawking, The Four laws of black hole mechanics, *Commun. Math. Phys.* **31**, 161 (1973).
- [6] D. N. Page, Hawking radiation and black hole thermodynamics, *New J. Phys.* **7**, 203 (2005), arXiv:hep-th/0409024.
- [7] K. D. Kokkotas and B. G. Schmidt, Quasinormal modes of stars and black holes, *Living Rev. Rel.* **2**, 2 (1999), arXiv:gr-qc/9909058.
- [8] H.-P. Nollert, Quasinormal modes: the characteristic ‘sound’ of black holes and neutron stars, *Class. Quant. Grav.* **16**, R159 (1999).
- [9] E. Berti, V. Cardoso, and A. O. Starinets, Quasinormal modes of black holes and black branes, *Class. Quant. Grav.* **26**, 163001 (2009), arXiv:0905.2975 [gr-qc].
- [10] R. A. Konoplya and A. Zhidenko, Quasinormal modes of black holes: From astrophysics to string theory, *Rev. Mod. Phys.* **83**, 793 (2011), arXiv:1102.4014 [gr-qc].
- [11] O. Dreyer, B. J. Kelly, B. Krishnan, L. S. Finn, D. Garrison, and R. Lopez-Aleman, Black hole spectroscopy: Testing general relativity through gravitational wave observations, *Class. Quant. Grav.* **21**, 787 (2004), arXiv:gr-qc/0309007.
- [12] E. Berti, V. Cardoso, and C. M. Will, On gravitational-wave spectroscopy of massive black holes with the space interferometer LISA, *Phys. Rev. D* **73**, 064030 (2006), arXiv:gr-qc/0512160.
- [13] E. Berti, J. Cardoso, V. Cardoso, and M. Cavaglia, Matched-filtering and parameter estimation of ring-down waveforms, *Phys. Rev. D* **76**, 104044 (2007), arXiv:0707.1202 [gr-qc].
- [14] E. Berti, A. Sesana, E. Barausse, V. Cardoso, and K. Belczynski, Spectroscopy of Kerr black holes with Earth- and space-based interferometers, *Phys. Rev. Lett.* **117**, 101102 (2016), arXiv:1605.09286 [gr-qc].
- [15] E. Berti, K. Yagi, H. Yang, and N. Yunes, Extreme Gravity Tests with Gravitational Waves from Compact Binary Coalescences: (II) Ringdown, *Gen. Rel. Grav.* **50**, 49 (2018), arXiv:1801.03587 [gr-qc].
- [16] R. Abbott *et al.* (LIGO Scientific, Virgo), Tests of general relativity with binary black holes from the second LIGO-Virgo gravitational-wave transient catalog, *Phys. Rev. D* **103**, 122002 (2021), arXiv:2010.14529 [gr-qc].
- [17] I. Ota and C. Chirenti, Overtones or higher harmonics? Prospects for testing the no-hair theorem with gravitational wave detections, *Phys. Rev. D* **101**, 104005 (2020), arXiv:1911.00440 [gr-qc].
- [18] E. Finch and C. J. Moore, Frequency-domain analysis of black-hole ringdowns, *Phys. Rev. D* **104**, 123034 (2021), arXiv:2108.09344 [gr-qc].
- [19] R. Cotesta, G. Carullo, E. Berti, and V. Cardoso, Analysis of Ringdown Overtones in GW150914, *Phys. Rev. Lett.* **129**, 111102 (2022), arXiv:2201.00822 [gr-qc].
- [20] R. Wald, Gedanken experiments to destroy a black hole, *Annals Phys.* **82**, 548 (1974).
- [21] V. E. Hubeny, Overcharging a black hole and cosmic censorship, *Phys. Rev. D* **59**, 064013 (1999), arXiv:gr-qc/9808043.
- [22] S. Hod, Cosmic censorship, area theorem, and selfenergy of particles, *Phys. Rev. D* **66**, 024016 (2002), arXiv:gr-qc/0205005.
- [23] T. Jacobson and T. P. Sotiriou, Over-spinning a black hole with a test body, *Phys. Rev. Lett.* **103**, 141101 (2009), [Erratum: *Phys.Rev.Lett.* 103, 209903 (2009)], arXiv:0907.4146 [gr-qc].
- [24] G. Chirco, S. Liberati, and T. P. Sotiriou, Gedanken experiments on nearly extremal black holes and the Third Law, *Phys. Rev. D* **82**, 104015 (2010), arXiv:1006.3655 [gr-qc].
- [25] J. Natario, L. Queimada, and R. Vicente, Test fields cannot destroy extremal black holes, *Class. Quant. Grav.* **33**, 175002 (2016), arXiv:1601.06809 [gr-qc].
- [26] J. Sorce and R. M. Wald, Gedanken experiments to destroy a black hole. II. Kerr-Newman black holes cannot be overcharged or overspun, *Phys. Rev. D* **96**, 104014 (2017), arXiv:1707.05862 [gr-qc].
- [27] M. Sasaki and T. Nakamura, Gravitational Radiation from Extreme Kerr Black Hole, *Gen. Rel. Grav.* **22**, 1351 (1990).
- [28] H. Onozawa, T. Mishima, T. Okamura, and H. Ishihara, Quasinormal modes of maximally charged black holes, *Phys. Rev. D* **53**, 7033 (1996), arXiv:gr-qc/9603021.
- [29] H. Nakano, N. Sago, T. Tanaka, and T. Nakamura, Estimate of the radius responsible for quasinormal modes in the extreme Kerr limit and asymptotic behavior of the Sasaki–Nakamura transformation, *PTEP* **2016**, 083E01 (2016), arXiv:1604.08285 [gr-qc].
- [30] S. Hod, Slow relaxation of rapidly rotating black holes, *Phys. Rev. D* **78**, 084035 (2008), arXiv:0811.3806 [gr-qc].
- [31] S. Aretakis, Decay of Axisymmetric Solutions of the Wave Equation on Extreme Kerr Backgrounds, *J. Funct. Anal.* **263**, 2770 (2012), arXiv:1110.2006 [gr-qc].
- [32] J. Lucietti and H. S. Reall, Gravitational instability of an extreme Kerr black hole, *Phys. Rev. D* **86**, 104030 (2012), arXiv:1208.1437 [gr-qc].
- [33] K. Murata, H. S. Reall, and N. Tanahashi, What happens at the horizon(s) of an extreme black hole?, *Class. Quant. Grav.* **30**, 235007 (2013), arXiv:1307.6800 [gr-qc].
- [34] S. E. Gralla, A. Zimmerman, and P. Zimmerman, Transient Instability of Rapidly Rotating Black Holes, *Phys. Rev. D* **94**, 084017 (2016), arXiv:1608.04739 [gr-qc].
- [35] B. Carneiro da Cunha and F. Novaes, Kerr Scat-

- tering Coefficients via Isomonodromy, *JHEP* **11**, 144, arXiv:1506.06588 [hep-th].
- [36] J. G. Rosa, The Extremal black hole bomb, *JHEP* **06**, 015, arXiv:0912.1780 [hep-th].
- [37] J. D. Schnittman, The Collisional Penrose Process, *Gen. Rel. Grav.* **50**, 77 (2018), arXiv:1910.02800 [astro-ph.HE].
- [38] D. Kapec and A. Lupsasca, Particle motion near high-spin black holes, *Class. Quant. Grav.* **37**, 015006 (2020), arXiv:1905.11406 [hep-th].
- [39] A. Strominger and C. Vafa, Microscopic origin of the Bekenstein-Hawking entropy, *Phys. Lett. B* **379**, 99 (1996), arXiv:hep-th/9601029.
- [40] A. Strominger, Black hole entropy from near horizon microstates, *JHEP* **02**, 009, arXiv:hep-th/9712251.
- [41] T. Jacobson, Semiclassical decay of near extremal black holes, *Phys. Rev. D* **57**, 4890 (1998), arXiv:hep-th/9705017.
- [42] M. Guica, T. Hartman, W. Song, and A. Strominger, The Kerr/CFT Correspondence, *Phys. Rev. D* **80**, 124008 (2009), arXiv:0809.4266 [hep-th].
- [43] T. Padmanabhan, Thermodynamical Aspects of Gravity: New insights, *Rept. Prog. Phys.* **73**, 046901 (2010), arXiv:0911.5004 [gr-qc].
- [44] I. Bredberg, T. Hartman, W. Song, and A. Strominger, Black Hole Superradiance From Kerr/CFT, *JHEP* **04**, 019, arXiv:0907.3477 [hep-th].
- [45] H. K. Kunduri and J. Lucietti, Classification of near-horizon geometries of extremal black holes, *Living Rev. Rel.* **16**, 8 (2013), arXiv:1306.2517 [hep-th].
- [46] G. E. A. Matsas and A. R. R. da Silva, Overspinning a nearly extreme charged black hole via a quantum tunneling process, *Phys. Rev. Lett.* **99**, 181301 (2007), arXiv:0706.3198 [gr-qc].
- [47] S. Hod, Weak Cosmic Censorship: As Strong as Ever, *Phys. Rev. Lett.* **100**, 121101 (2008), arXiv:0805.3873 [gr-qc].
- [48] G. E. A. Matsas, M. Richartz, A. Saa, A. R. R. da Silva, and D. A. T. Vanzella, Can quantum mechanics fool the cosmic censor?, *Phys. Rev. D* **79**, 101502 (2009), arXiv:0905.1077 [gr-qc].
- [49] N. Andersson and K. Glampedakis, A Superradiance resonance cavity outside rapidly rotating black holes, *Phys. Rev. Lett.* **84**, 4537 (2000), arXiv:gr-qc/9909050.
- [50] K. Glampedakis and N. Andersson, Late time dynamics of rapidly rotating black holes, *Phys. Rev. D* **64**, 104021 (2001), arXiv:gr-qc/0103054.
- [51] V. Cardoso, A Note on the resonant frequencies of rapidly rotating black holes, *Phys. Rev. D* **70**, 127502 (2004), arXiv:gr-qc/0411048.
- [52] S. Hod, Quasinormal resonances of a massive scalar field in a near-extremal Kerr black hole spacetime, *Phys. Rev. D* **84**, 044046 (2011), arXiv:1109.4080 [gr-qc].
- [53] H. Yang, F. Zhang, A. Zimmerman, D. A. Nichols, E. Berti, and Y. Chen, Branching of quasinormal modes for nearly extremal Kerr black holes, *Phys. Rev. D* **87**, 041502 (2013), arXiv:1212.3271 [gr-qc].
- [54] H. Yang, A. Zimmerman, A. Zenginoglu, F. Zhang, E. Berti, and Y. Chen, Quasinormal modes of nearly extremal Kerr spacetimes: spectrum bifurcation and power-law ringdown, *Phys. Rev. D* **88**, 044047 (2013), arXiv:1307.8086 [gr-qc].
- [55] G. B. Cook and M. Zalutskiy, Gravitational perturbations of the Kerr geometry: High-accuracy study, *Phys. Rev. D* **90**, 124021 (2014), arXiv:1410.7698 [gr-qc].
- [56] M. Richartz, Quasinormal modes of extremal black holes, *Phys. Rev. D* **93**, 064062 (2016), arXiv:1509.04260 [gr-qc].
- [57] B. Carneiro da Cunha and J. P. Cavalcante, Teukolsky master equation and Painlevé transcendents: Numerics and extremal limit, *Phys. Rev. D* **104**, 084051 (2021), arXiv:2105.08790 [hep-th].
- [58] M. Casals, S. E. Gralla, and P. Zimmerman, Horizon Instability of Extremal Kerr Black Holes: Nonaxisymmetric Modes and Enhanced Growth Rate, *Phys. Rev. D* **94**, 064003 (2016), arXiv:1606.08505 [gr-qc].
- [59] M. Richartz, C. A. R. Herdeiro, and E. Berti, Synchronous frequencies of extremal Kerr black holes: resonances, scattering and stability, *Phys. Rev. D* **96**, 044034 (2017), arXiv:1706.01112 [gr-qc].
- [60] M. Casals and L. F. Longo Micchi, Spectroscopy of extremal and near-extremal Kerr black holes, *Phys. Rev. D* **99**, 084047 (2019), arXiv:1901.04586 [gr-qc].
- [61] T. J. M. Zouros and D. M. Eardley, Instabilities of Massive Scalar Perturbations of a Rotating Black Hole, *Annals Phys.* **118**, 139 (1979).
- [62] S. L. Detweiler, Klein-Gordon Equation and Rotating Black Holes, *Phys. Rev. D* **22**, 2323 (1980).
- [63] S. R. Dolan, Instability of the massive Klein-Gordon field on the Kerr spacetime, *Phys. Rev. D* **76**, 084001 (2007), arXiv:0705.2880 [gr-qc].
- [64] S. R. Dolan, Superradiant instabilities of rotating black holes in the time domain, *Phys. Rev. D* **87**, 124026 (2013), arXiv:1212.1477 [gr-qc].
- [65] S. Hod, Stationary Scalar Clouds Around Rotating Black Holes, *Phys. Rev. D* **86**, 104026 (2012), [Erratum: *Phys. Rev. D* **86**, 129902 (2012)], arXiv:1211.3202 [gr-qc].
- [66] C. A. R. Herdeiro and E. Radu, Kerr black holes with scalar hair, *Phys. Rev. Lett.* **112**, 221101 (2014), arXiv:1403.2757 [gr-qc].
- [67] A. Arvanitaki, S. Dimopoulos, S. Dubovsky, N. Kaloper, and J. March-Russell, String Axiverse, *Phys. Rev. D* **81**, 123530 (2010), arXiv:0905.4720 [hep-th].
- [68] A. Arvanitaki and S. Dubovsky, Exploring the String Axiverse with Precision Black Hole Physics, *Phys. Rev. D* **83**, 044026 (2011), arXiv:1004.3558 [hep-th].
- [69] R. Brito, V. Cardoso, and P. Pani, Superradiance: New Frontiers in Black Hole Physics, *Lect. Notes Phys.* **906**, pp.1 (2015), arXiv:1501.06570 [gr-qc].
- [70] T. Kato, *Perturbation Theory for Linear Operators*, Grundlehren der mathematischen Wissenschaften, Vol. 132 (Springer, 1995).
- [71] M. V. Berry, Physics of Nonhermitian Degeneracies, *Czech. J. Phys.* **54**, 1039 (2004).
- [72] E. J. Bergholtz, J. C. Budich, and F. K. Kunst, Exceptional topology of non-Hermitian systems, *Rev. Mod. Phys.* **93**, 015005 (2021), arXiv:1912.10048 [cond-mat.mes-hall].
- [73] M.-A. Miri and A. Alù, Exceptional points in optics and photonics, *Science* **363**, eaar7709 (2019), <https://www.science.org/doi/pdf/10.1126/science.aar7709>.
- [74] K. Ding, C. Fang, and G. Ma, Non-Hermitian topology and exceptional-point geometries, *Nature Rev. Phys.* **4**, 745 (2022), arXiv:2204.11601 [quant-ph].
- [75] D. R. Brill, P. L. Chrzanowski, C. Martin Pereira, E. D. Fackerell, and J. R. Ipser, Solution of the scalar wave equation in a kerr background by separation of variables, *Phys. Rev. D* **5**, 1913 (1972).

- [76] J. N. Goldberg, A. J. Macfarlane, E. T. Newman, F. Rohrlich, and E. C. G. Sudarshan, Spin-s Spherical Harmonics and δ , *Journal of Mathematical Physics* **8**, 2155 (1967).
- [77] E. Berti, V. Cardoso, and M. Casals, Eigenvalues and eigenfunctions of spin-weighted spheroidal harmonics in four and higher dimensions, *Phys. Rev. D* **73**, 024013 (2006).
- [78] D. Batic and H. Schmid, Heun equation, Teukolsky equation, and type-D metrics, *J. Math. Phys.* **48**, 042502 (2007), arXiv:gr-qc/0701064.
- [79] P. P. Fiziev, Classes of Exact Solutions to the Teukolsky Master Equation, *Class. Quant. Grav.* **27**, 135001 (2010), arXiv:0908.4234 [gr-qc].
- [80] A. Ronveaux and F. Arscott, *Heun's Differential Equations*, Oxford science publications (Oxford University Press, 1995).
- [81] S. Slavianov and W. Lay, *Special Functions: A Unified Theory Based on Singularities*, Oxford Science Publications (Oxford University Press, 2000).
- [82] E. Leaver, An Analytic representation for the quasi normal modes of Kerr black holes, *Proc.Roy.Soc.Lond.* **A402**, 285 (1985).
- [83] H.-P. Nollert, Quasinormal modes of Schwarzschild black holes: The determination of quasinormal frequencies with very large imaginary parts, *Phys. Rev. D* **47**, 5253 (1993).
- [84] O. Gamayun, N. Iorgov, and O. Lisovyy, How instanton combinatorics solves Painlevé VI, V and IIIs, *J.Phys.* **A46**, 335203 (2013), 1302.1832.
- [85] B. Carneiro da Cunha and J. P. Cavalcante, Expansions for semiclassical conformal blocks, *Journal of High Energy Physics* **08**, 110 (2024), arXiv:2211.03551 [hep-th].
- [86] J. P. Cavalcante, M. Richartz, and B. Carneiro da Cunha, Massive scalar perturbations in Kerr Black Holes: near extremal analysis, (2024), arXiv:2408.13964 [gr-qc].
- [87] M. Casals, A. C. Ottewill, and N. Warburton, High-order asymptotics for the Spin-Weighted Spheroidal Equation at large real frequency, *Proc. Roy. Soc. Lond. A* **475**, 20180701 (2019), arXiv:1810.00432 [gr-qc].
- [88] J. P. Cavalcante, M. Richartz, and B. Carneiro da Cunha, Data and scripts for: "Exceptional point and hysteresis in perturbations of Kerr black holes" and "Massive scalar perturbations in Kerr Black Holes: near extremal analysis", 10.5281/zenodo.13961216 (2024).
- [89] J. P. Cavalcante and B. Carneiro da Cunha, Scalar and Dirac perturbations of the Reissner-Nordström black hole and Painlevé transcendents, *Phys. Rev. D* **104**, 124040 (2021), arXiv:2109.06929 [gr-qc].
- [90] R. A. Konoplya and A. Zhidenko, Stability and quasinormal modes of the massive scalar field around Kerr black holes, *Phys. Rev. D* **73**, 124040 (2006), arXiv:gr-qc/0605013.
- [91] R. A. Konoplya and A. Zhidenko, Massive charged scalar field in the Kerr-Newman background I: quasinormal modes, late-time tails and stability, *Phys. Rev. D* **88**, 024054 (2013), arXiv:1307.1812 [gr-qc].
- [92] P. H. C. Siqueira and M. Richartz, Quasinormal modes, quasibound states, scalar clouds, and superradiant instabilities of a Kerr-like black hole, *Phys. Rev. D* **106**, 024046 (2022), arXiv:2205.00556 [gr-qc].
- [93] M. Richartz, J. L. Rosa, and E. Berti, Bounds on the mass of superradiantly unstable scalar fields around Kerr black holes, (2024), arXiv:2405.01003 [gr-qc].
- [94] O. Lisovyy, H. Nagoya, and J. Roussillon, Irregular conformal blocks and connection formulae for Painlevé V functions, *J. Math. Phys.* **59**, 091409 (2018), arXiv:1806.08344 [math-ph].
- [95] H. B. Callen, *Thermodynamics and an Introduction to Thermostatistics*, 2nd ed. (Wiley, 1991).
- [96] H. Motohashi, Resonant excitation of quasinormal modes of black holes, (2024), arXiv:2407.15191 [gr-qc].
- [97] O. J. C. Dias, M. Godazgar, J. E. Santos, G. Carullo, W. Del Pozzo, and D. Laghi, Eigenvalue repulsions in the quasinormal spectra of the Kerr-Newman black hole, *Phys. Rev. D* **105**, 084044 (2022), arXiv:2109.13949 [gr-qc].
- [98] O. J. C. Dias, M. Godazgar, and J. E. Santos, Eigenvalue repulsions and quasinormal mode spectra of Kerr-Newman: an extended study, *JHEP* **07**, 076, arXiv:2205.13072 [gr-qc].
- [99] A. Davey, O. J. C. Dias, and J. E. Santos, Scalar QNM spectra of Kerr and Reissner-Nordström revealed by eigenvalue repulsions in Kerr-Newman, *JHEP* **12**, 101, arXiv:2305.11216 [gr-qc].